Deep crustal structure of the Adare and Northern Basins, Ross Sea, Antarctica, from sonobuoy data

M.M. Selvans [a,b,*], J.M. Stock [a], R.W. Clayton [a], S. Cande [c], R. Granot [d]

[a] *Seismological Laboratory, California Institute of Technology, 1200 E. California Blvd., MC 252-21, Pasadena, CA 91125, United States*
[b] *Center for Earth and Planetary Studies, National Air and Space Museum, Smithsonian Institution, 4th St. SW and Independence Ave., MRC 315, Washington, DC 20013, United States*
[c] *Scripps Institution of Oceanography, MC 0220, La Jolla, CA 92093, United States*
[d] *Department of Geological and Environmental Sciences, Ben-Gurion University of the Negev, Beer Sheva, Israel*

A B S T R A C T

Extension associated with ultraslow seafloor spreading within the Adare Basin, in oceanic crust just north of the continental shelf in the Ross Sea, Antarctica, extended south into the Northern Basin. Magnetic and gravity anomaly data suggest continuity of crustal structure across the continental shelf break that separates the Adare and Northern Basins. We use sonobuoy refraction data and multi-channel seismic (MCS) reflection data collected during research cruise NBP0701, including 71 new sonobuoy records, to provide constraints on crustal structure in the Adare and Northern Basins. Adjacent 1D sonobuoy profiles along several MCS lines reveal deep crustal structure in the vicinity of the continental shelf break, and agree with additional sonobuoy data that document fast crustal velocities (6000–8000 m/s) at shallow depths (1–6 km below sea level) from the Adare Basin to the continental shelf, a structure consistent with that of other ultraslow-spread crust. Our determination of crustal structure in the Northern Basin only extends through sedimentary rock to the basement rock, and so cannot help to distinguish between different hypotheses for formation of the basin.

© 2014 Elsevier B.V. All rights reserved.

1. Introduction

Deformation processes by which extensional strain at mid-ocean ridges, in relatively thin and dense oceanic crust, is transferred to neighboring continental crust are poorly understood. The breakup of Gondwana during Cretaceous time produced the West Antarctic Rift System (WARS) within continental crust (e.g., Elliot, 1992), which makes up the majority of the crust in the Ross Sea. The WARS is tectonically complex and difficult to study due to being largely covered by an ice sheet and sea ice, and because much of the rifting took place within continental crust at extremely slow rates, making it the least well constrained link in the global plate circuit.

During mid-Cenozoic time, seafloor spreading occurred for 17 million years (43–26 Ma) at the Adare Basin (Cande et al., 2000), producing oceanic crust in the northwesternmost Ross Sea (Fig. 1). The Adare spreading center lies in the deep water of the Adare

Basin and trends southward toward the Northern Basin, which is a structurally-defined feature on the continental shelf (e.g., Cooper et al., 1995). Magnetic anomalies are used to constrain the timing and spreading rate of the Adare spreading center (Cande et al., 2000); two of these magnetic anomalies are continuous with similarly strong and narrow magnetic features that extend into the neighboring continental shelf of the Northern Basin (Granot et al., 2013; Damaske et al., 2007; Cande and Stock, 2006). Multi-channel seismic (Granot et al., 2010; Müller et al., 2005; Brancolini et al., 1995), sonobuoy (Cooper et al., 1987; Houtz and Davey, 1973), and Deep Sea Drilling Project (Hayes et al., 1975a, 1975b) studies have characterized the shallow crustal structure at a few locations in the vicinity.

In this paper we present the analysis of sonobuoy data collected during research cruise NBP0701 on board the *R/VIB Nathaniel B. Palmer* (Adare Basin Sonobuoy Data, 2007; NBP0701 Data Report, 2007), in the Adare and Northern Basins (shown with respect to bathymetry, magnetic anomalies, and free-air gravity anomalies in Fig. 2a–c). This is a companion paper to the analysis by Granot et al. (2010) of the multi-channel seismic (MCS) reflection data from the same cruise. While MCS data are useful for determining the velocity of the shallowest rock layer, sonobuoy data allow us to directly measure layer velocities at depth (see Selvans et al., 2012).

* Corresponding author at: Center for Earth and Planetary Studies, National Air and Space Museum, Smithsonian Institution, 4th St. and Independence Ave. SW, MRC 315, Washington, DC 20024, United States. Tel.: +1 202 633 2476.
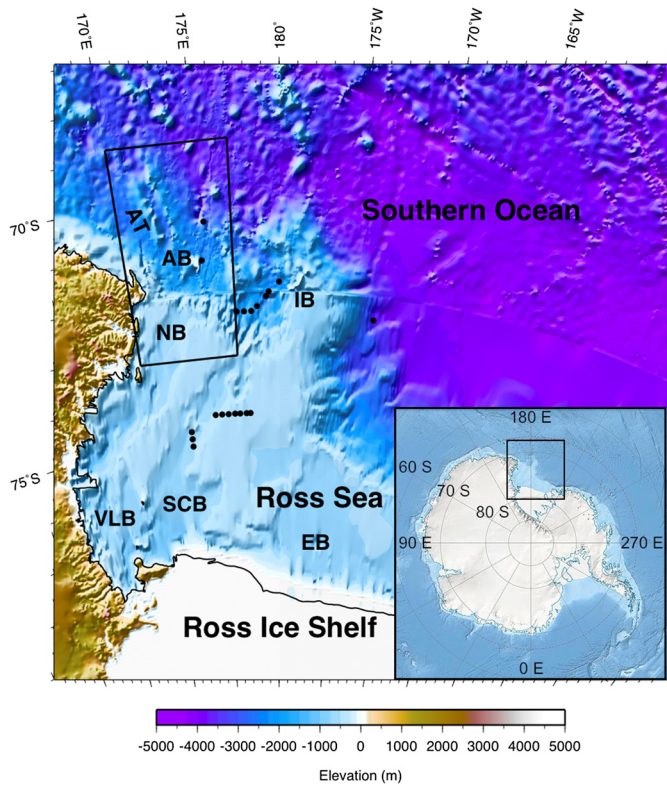   *E-mail address:* selvansm@si.edu (M.M. Selvans).

Fig. 1. Bathymetry of the Ross Sea and Southern Ocean shows a clear delineation of the continental shelf. Our study area (black box) lies at one end of the West Antarctic Rift System, in the northwestern-most Ross Sea. To the east of our study area, the continental crust of Iselin Bank (IB) juts out into oceanic crust. Sonobuoy data from previous studies (black dots) are discussed in the text. Key features are labeled: Adare Basin (AB), Adare Trough (AT), Northern Basin (NB), Victoria Land Basin (VLB), Southern Central Basin (SCB), Eastern Basin (EB). Shuttle Radar Topography Mission data and estimated seafloor bathymetry are ~1 km resolution (Becker and Sandwell, 2006). Inset is the location of this figure with respect to Antarctica.

The 71 sonobuoy profiles presented here, deployed along the 19 MCS lines, provide a deeper and more detailed look at the crust in the Adare and Northern Basins than was possible in prior studies of this region.

1.1. Tectonic history of the northwestern Ross Sea

During the final stages of breakup of Gondwana in mid-Cretaceous time (~100 Ma), the Ross Sea margin of Antarctica rifted from the Campbell Plateau and the South Tasman Rise, the former bordering Marie Byrd Land (West Antarctica) and most of the Ross Sea continental margin, and the latter adjacent to the westernmost Ross Sea and Cape Adare of East Antarctica (e.g., Weaver et al., 1994). Tectonic reconstructions (e.g., Cande et al., 1995) and crustal structure (Cooper et al., 1987) suggest that Iselin Bank is continental material that may have been part of East Antarctica (see Fig. 1).

While Gondwana was breaking up, rifting began between East and West Antarctica along the WARS. At ~90 Ma, the South Tasman Rise was close to East Antarctica and the Iselin Bank (Gaina et al., 1998). Since the mid-Cretaceous, 500–1000 km of broadly distributed transtensional motion has occurred within the WARS (Luyendyk et al., 1996). Extension between the South Tasman Rise and East Antarctica began ~ 60 Ma, rifting slowly, while ~300 km of extension between East and West Antarctica occurred between 80 and 40 Ma (Cande et al., 2000; Molnar et al., 1975). Marine sedimentary rocks from the eastern Ross Sea are Eocene in age (57–35 Ma), consistent with the formation of sediment-

accumulating basins due to extension during this time (Truswell and Drewry, 1984).

Additionally, in the western Ross Sea north–south trending basins and ridges formed during periods of extension in late Cretaceous and early Cenozoic time (Cooper et al., 1987; Decesari et al., 2007). In particular, at ~60 Ma the Iselin Bank was adjacent to Cape Adare, whereas by ~27 Ma it had moved to its current position, accommodating extension north of the Ross Sea, creating the Adare Basin and significantly deforming the continental crust at its southern edge, where the Northern Basin now lies (Cande and Stock, 2004).

The western Ross Sea has also experienced distributed volcanic and tectonic deformation since mid-Cenozoic time. Extension and subsidence formed the Victoria Land and Northern Basins (Cooper and Davey, 1985; Davey et al., 2006). Extension was concentrated in the Adare Basin when seafloor spreading took place from 43 to 26 Ma (Cande et al., 2000). Recent minor extensional episodes at ~24 Ma and ~17 Ma have resulted in the formation of the Adare Trough (Granot et al., 2010). Finally, ongoing deformation has disrupted the sedimentary rocks that were deposited on top of the Adare Basin oceanic crust (Granot et al., 2010). Young Pliocene volcanic knolls on the continental shelf and in the deep water offshore from Cape Adare, which are similar in composition to other volcanoes in the western Ross Sea (Panter and Castillo, 2007), postdate formation of the Adare Basin oceanic crust (Granot et al., 2010; Panter and Castillo, 2007). Features in magnetic, gravity, and MCS data are not offset across the boundary between the Adare and Northern Basins, indicating that these basins are structurally continuous (Cande and Stock, 2006; Damaske et al., 2007).

1.2. Multi-channel seismic data in the Adare and Northern Basins

MCS data collected during research cruise NBP0701 (see Fig. 2) have resolvable primary reflections up to 2.2 s of (two-way) travel time in the continental shelf (Granot et al., 2010). Several sedimentary rock horizons can be continuously traced throughout the region. The thickness of sedimentary cover generally ranges from 0 s in travel time along the ridges bounding the Adare Trough to 2.0 s at one point within the Adare Trough, and reach their thickest (>2.2 s) in the Northern Basin and the margin slope (Granot et al., 2010).

1.3. Previous seismic refraction studies in the Ross Sea

Seismic refraction data collected in the Ross Sea provide clues to the deep crustal structure of the basins and ridges therein. In the central and southern Ross Sea (near the Ross Ice Shelf), ocean bottom seismometers were used to obtain the deepest crustal structure studies in the region. Mantle velocities (>8.0 km/s) were detected at a minimum depth of 16 km below the seafloor (Trey et al., 1999), and basement rock was detected as thin as ~5 km, with ~7 km of overlying sediment and an underlying layer of ~7 km of inferred magmatic intrusions (Tréhu et al., 1993). However, only sonobuoys have been deployed near our study area.

Ten sonobuoys deployed in shallow water just south of our study area (see locations in Fig. 1) detected maximum sedimentary rock velocities >4.0 km/s, basement velocities of 5.0–5.8 km/s, and assumed basement depths of 1.0–1.6 km subseafloor (Houtz and Davey, 1973). Six sonobuoys in deep water along the continental shelf between the Northern Basin and the Iselin Bank, just east of our study area, revealed maximum sedimentary rock velocities up to 4.3 km/s, assumed basement velocities up to 4.7 km/s, and basement depths of up to 3.0 km subseafloor (Houtz and Davey, 1973). However, a similar study nearby (Cooper et al., 1987) indicated that many velocities >4.9 km/s are in fact layered sedimentary
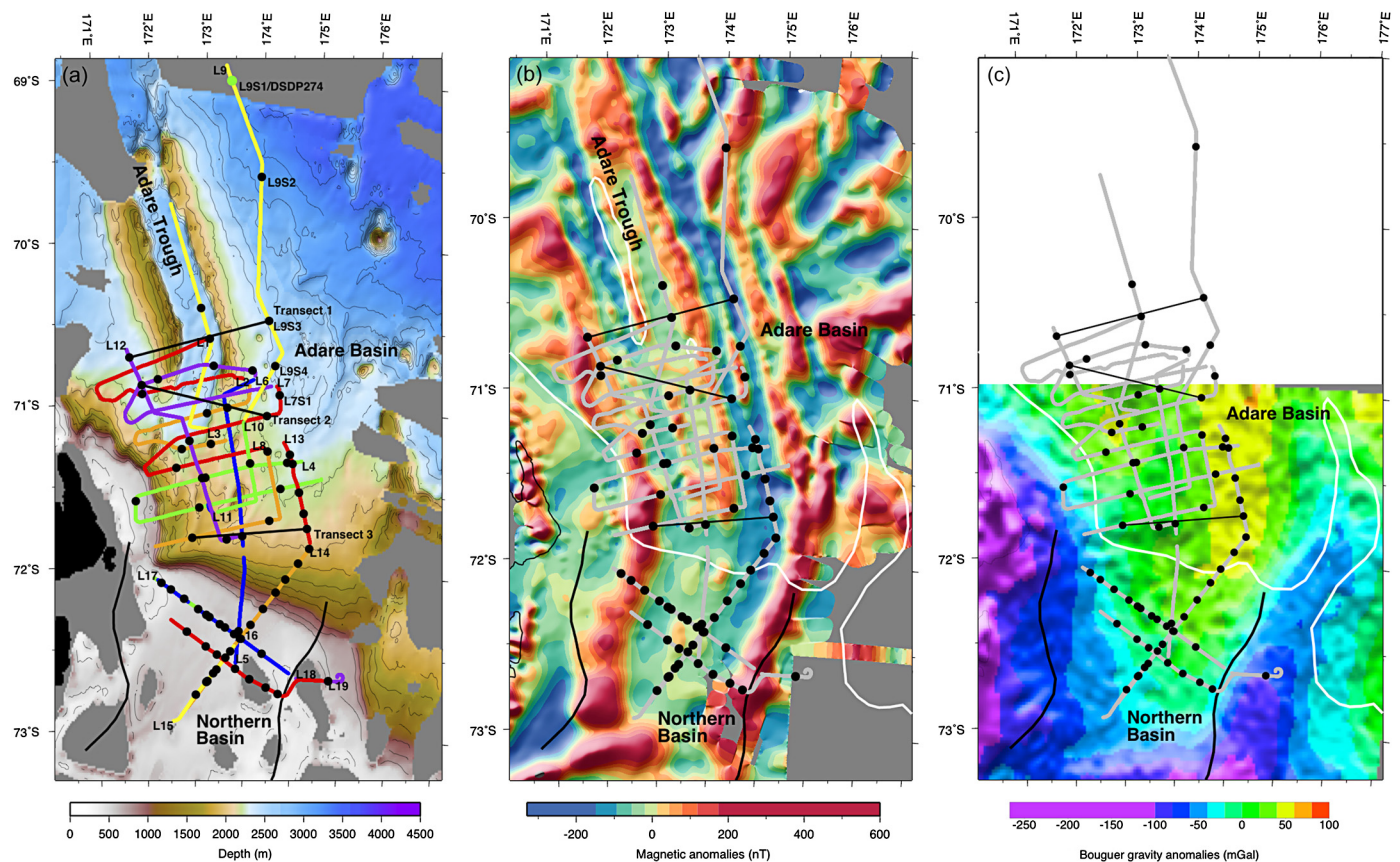
Fig. 2. We investigate crustal structure using multi-channel seismic (MCS) and sonobuoy data from research cruise NBP0701. (a) The Adare Basin lies in deep water north of the continental shelf break, whereas the Northern Basin (within the sinuous black lines, after Cande et al., 2000) extends from the shelf break to 73.5°S. Locations of MCS lines (colored lines, labeled at the beginning of the line) (NBP0701 Data Report, 2007) and sonobuoys (black dots) are displayed on top of multibeam bathymetry (Adare Basin Sonobuoy Data, 2007). See Section 3.2 of the text for additional clarification of MCS line locations on the continental shelf; sonobuoys are depicted sequentially from the start of each MCS line, following the example of line L9. Deep Sea Drilling Project site (DSDP) 274 (green dot) is collocated with sonobuoy L9S1. (b) Compiled shipboard magnetic (Cande et al., 2000; Cande and Stock, 2006) and aeromag data (Damaske et al., 2007) show that magnetic anomalies are continuous across the continental shelf (Granot et al., 2013). (c) There is no correspondence between bouguer gravity anomalies and the continental shelf break; gravity data (Sandwell and Smith, 2009) are corrected for water depth and basement-sediment depth of Davey and Brancolini (1995) (which is known only as far north as 71.0°S). MCS line, transect, and sonobuoy locations are overlain in gray and black in (b) and (c); 1500 m water depth is shown as a white contour.

rock units and not igneous-metamorphic basement, so the above basement depths may be an underestimate.

Additional sonobuoys deployed over the Iselin Bank and in the deep water to its east and west indicate that the Iselin Bank is composed of continental crust, with oceanic crust ∼10 km thick to its east (Cooper et al., 1987). West of Iselin Bank, just east of our study area, a velocity of 5.2 km/s was detected at 4.3 km subseafloor depth, and similar velocities were detected at 1.8 and 2.8 km subseafloor depth in the Adare Basin (at 70.7°S, 175.3°E, and 71.3°S, 175.0°E, respectively) (Cooper et al., 1987).

In the southern Ross Sea, sonobuoys revealed a range of velocity gradients similar to those found in sedimentary rocks further north (Cochrane et al., 1995; Davey et al., 1983, 1982); Ross Sea sedimentary rock velocities are systematically faster than those found at similar depths in the Gulf of Alaska (e.g., Bruns and Carlson, 1987) and the Gulf of Mexico (e.g., Gardner et al., 1974). This is interpreted as the result of compaction of Ross Sea sediments due to past loading by a grounded ice sheet (Cochrane et al., 1995). Similarly fast sedimentary rock layer velocities at shallow depths in the northern Svalbard margin are also attributed to ice loading (Geissler and Jokat, 2004).

2. Sonobuoy analysis methods

MCS data were recorded with a 1.2 km, 48-channel streamer. Lines 1–12, in deeper water, used a 6-gun G/I source array with a total capacity of 20.6 l. For seismic Lines 13–19, on and near the continental shelf, we used a 6-element Bolt-gun array with a total capacity of 34.8 l. The typical source spacing was approximately 40 m. Sonobuoys were deployed occasionally in deep water, and with a regular spacing of ∼15 km in shallow water (see Fig. 2). Most sonobuoys provided data until they were 20–30 km away from the ship. We use MCS data to constrain the velocity of the shallowest rock layer, and sonobuoy data to reveal velocity profiles deep into the oceanic crust. We assume planar layers for all velocity horizons, consistent with the linear segmented travel time plots and the generally flat horizons observed in the MCS data.

We confirm our 1D velocity models for each sonobuoy profile through finite difference modeling and depth migration of the data (Selvans et al., 2012). Smoothed and interpolated adjacent sonobuoy profiles along MCS Lines 13–19 allow us to also construct 2D velocity models, as do the more widely spaced sonobuoys along Transect 3 in the Adare Basin ('transects' are lines along which we analyze trends in crustal structure, even though they do not coincide with lines of MCS data, shown in black in Fig. 2). We use a Delaunay triangulation algorithm for the interpolation, with location (depth below seafloor and distance along the line) and velocity as vertices (Selvans et al., 2012).

3. Results of 1D and 2D velocity models

3.1. Deep structure in the Adare Basin

MCS Lines 1–13 provide good coverage of the Adare Basin; 36 sonobuoys deployed along these lines reveal the deep structure of the crust from the southern end of the Adare Trough to the continental shelf at the north end of the Northern Basin. These sonobuoys are generally spaced further apart from each other (>30 km) than the offsets from the ship to which they recorded data (20–30 km), and so provide 1D velocity models.

Sonobuoys in the Adare Basin record head waves from layers at maximum depths of 0.5–5.4 km below the seafloor; 28 of the 36 penetrate >2.0 km. These sonobuoy profiles reveal variable-thickness sedimentary layers (in agreement with MCS data; Granot et al., 2010) on top of basement rock, in four cases with maximum velocities of 7000–7400 m/s at 3.0–5.4 km below the seafloor (for example, see L7S1 in Fig. 5e). In another 15 sonobuoy profiles, maximum layer velocities of 6000–7000 m/s are observed at similar depths (see Table 1, Supplemental Material). Velocities are uncertain to ±100 m/s and depths are uncertain up to ±0.4 km (increasing with depth).

To aid in visualizing the trends in these 1D velocity models, we provide a 2D velocity model (see Section 2) along Transect 3 through the southern Adare Basin (Fig. 4). We also provide a comparison of 1D velocity models along Line 9 (Fig. 5), which runs along the eastern side of the Adare Trough, and along Transects 1 and 2 in the northern and middle Adare Basin (Supplemental Figs. S2 and S3, respectively). These sonobuoys are widely and irregularly spaced (23–60 km apart) and were collected along different azimuths (between the ship and receiver). The 2D velocity model along Transect 3 (Fig. 4) is accurate within ~5 km of each sonobuoy location (along the transect); further from the sonobuoy location, velocity contour depth varies from the same contour depth at the sonobuoy location by more than ±0.4 km (the velocity vertical uncertainty). Apparently dipping velocity contours result from the interpolation process rather than from direct measurements of the sonobuoy data, and shallow structure between sonobuoy locations (as observed in nearby MCS data) is not represented.

Transect 1 crosses the southern Adare Trough roughly perpendicular to its axis (see Fig. 2 for transect location, and Fig. S2a–c for 1D velocity profiles); nearby MCS data shows sediment layers wedging out against the trough flanks (Fig. S2d). Relatively fast velocities (4600–6000 m/s) are observed deeper in the middle of this transect, where sonobuoy L3S2 (Fig. S2b) detects the crustal structure within the Adare Trough. All three sonobuoys reveal simple three-layer structure, with maximum velocities (from west to east) of 6500 m/s, 5000 m/s, and 5400 m/s (Fig. S2a–c).

Transect 2 also crosses the Adare Trough roughly perpendicular to its axis, and is at an angle to Transect 1 due to a change in azimuth of the Adare Trough (see Fig. 2 for context, and Fig. S3 for velocity profiles). In Transect 2, one sonobuoy profile lies to the west of the trough and two lie to its east; again sediment layers wedge out against trough flanks (Granot et al., 2010). These sonobuoys show slow velocities (up to 4000 m/s, likely consolidated sediment) at greater depth on the west side of the trough than on its east side. However, faster velocities (up to 6000 m/s, likely basement rock) are detected at the same depth on the east and west sides. At the two ends of this transect, sonobuoys L12S2 (Fig. S3a) and L7S2 (Fig. S3c) reveal maximum velocities of 6500 m/s and 7400 m/s, respectively. The latter value is the fastest layer velocity detected in the Adare Basin, and is typical of lower oceanic crust (e.g., Jones, 1999).

The 2D velocity model along Transect 3 (Fig. 4a) runs along the base of the continental shelf separating the Adare and North-ern Basins (see Fig. 2 for transect location). The fastest velocity contours (5000–5600 m/s) dip down slightly to the west, while slower-velocity contours deepen in the middle. The two sonobuoys closest to the continental shelf (L8S3 and L12S6; Figs. 4b and 4c) detect the deepest layers with velocities <6000 m/s observed in the Adare Basin (5700 m/s and 5300 m/s, at depths of 4.1 km and 4.3 km below the seafloor, respectively).

Sonobuoys along the trend of MCS Line 9 (four on that line, and L7S1) span the length of the Adare Trough, from Deep Sea Drilling Project (DSDP) site 274 to the north (collocated with sonobuoy L9S1) to the change in trough azimuth to the south (see Fig. 2). From north to south (Fig. 5a–e), these sonobuoy profiles have maximum layer velocities of 6800 m/s, 5900 m/s, 5400 m/s, 6000 m/s, and 7000 m/s, with relatively shallow depths for these layers of 0.7 km, 1.3 km, 2.0 km, 1.4 km, and 3.1 km below the seafloor (corresponding to 3.9, 4.3, 4.0, 3.7, and 5.4 km below sea level, respectively). Sonobuoy data on Line 9 detect only two or three layers, similarly to sonobuoy data along Transect 1. In contrast, sonobuoy L7S1 detects five layers, typical of sonobuoys south of Transect 1 in the Adare Basin that detect velocities >5000 m/s (of the 24 sonobuoys that match these criteria, 21 detect four to seven layers).

Within the Adare Basin, adjacent sonobuoy profiles were collected only along MCS Line 13, while approaching the continental shelf from the north. The 2D velocity model constructed from these five sonobuoy profiles (Fig. 6) reveals a crustal structure that is consistent with the eastern end of Transect 2, which is based on a sonobuoy from Line 7. The 2D velocity model for Line 13 indicates that the southern Adare Basin has horizontal velocity contours. Below the seafloor, which is the top of the rock layer with 2000 m/s velocity, contours of 3000 m/s, 4200 m/s, 4900 m/s, 5700 m/s, and 6000 m/s lie at subseafloor depths of ~0.6 km, ~1.8 km, ~2.3 km, ~3.1 km, and ~3.3 km respectively.

3.2. Deep structure across the continental shelf and in the Northern Basin

The crustal structure of the continental shelf and the Northern Basin is explored in detail, because adjacent sonobuoy profiles along MCS Lines 14–19 (see Fig. 2) allow for construction of three 2D velocity models. Line 14 trends northeast to southwest, approximately perpendicular to the trend of the shelf break between the Adare and Northern Basins, while Line 15 doubles back on the southern half of Line 14 (on the continental shelf). Line 17 doubles back on Line 16 (blue and green lines in Fig. 2a), crossing Lines 14 and 15 at a right angle within the Northern Basin. Line 19 (southernmost red line in Fig. 2a) runs parallel to Lines 16 and 17, and crosses Lines 14 and 15 (orange and yellow lines) another ~20 km further southwest.

The 2D velocity model that crosses the continental shelf, constructed from fourteen sonobuoy profiles along Lines 14 and 15, shows remarkably horizontal fast (>5000 m/s) velocity contours (within depth uncertainties; Fig. 7), similar to the 2D velocity model along Line 13. Depths of slower velocity contours (up to ~5000 m/s) agree between the two models; the 6000 m/s velocity contour is ~4.0 km below the seafloor along Lines 14, ~0.7 km deeper than the same contour where it is linearly interpolated along Line 13 (a reasonable difference relative to the depth uncertainty of ±0.4 km, since sonobuoys L13S6 and L14S1 are far enough apart to be sampling slightly different subsurface structure).

The only potential detection of the Moho in this study lies at the northern end of Line 14 (sonobuoy L14S1, see Table 1, Supplementary Material), where a velocity of 8000 ± 100 m/s originates at a depth of 5.5 ± 0.4 km below the seafloor (see also Selvans et al., 2012). In order to verify that this possible Moho detection
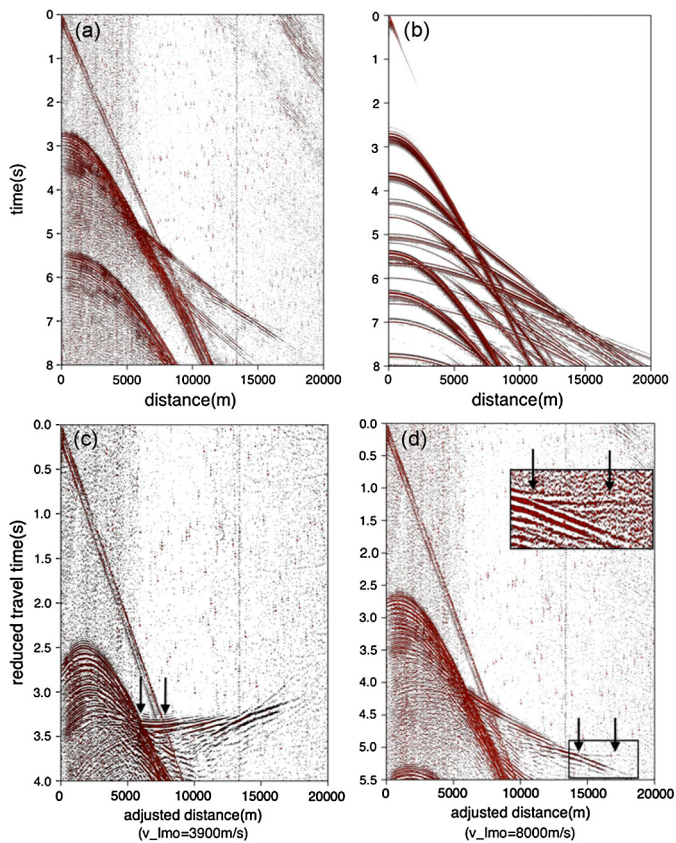
Fig. 3. Analysis and modeling of one sonobuoy incorporated in Fig. 7 (L14S1). The raw data (a) and finite difference model (b) show the direct wave (between the source and the receiver) as a straight line through the origin, curved reflections from layer interfaces (in (a), only the seafloor and its multiple are distinct, whereas in (b) other subsurface interfaces are also apparent), and head waves. Layer velocities are determined by applying a linear moveout (lmo) to each head wave, shown here for the first (c) and fourth (d) head waves in this record. See Supplemental Fig. S1 for the resulting 1D velocity profile. Adapted from Figs. 4 and 8 in Selvans et al. (2012).

is not a wide-angle reflection caused by basement topography, we used topography along interfaces imaged by MCS data (Granot et al., 2010), which correspond to layers detected by sonobuoy L14S1, to run a 2D finite difference model. We found no detectable difference between the 2D and 1D models for sonobuoy L14S1. We do however note that imaging based on MCS data is only available down to the basement (which corresponds to the L14S1 sonobuoy layer with velocity 4400 m/s, see Fig. 3), and that the 8000 m/s arrival is the result of an interface located substantially below this depth. Energy refracted off an up-dip interface with either serpentenized mantle (with layer velocity ∼7700 m/s; Ritzmann et al., 2004) or lower oceanic crust (velocity ∼7400 m/s; Jones, 1999, p. 342) could produce an apparent velocity of 8000 ± 100 m/s.

Of the other sonobuoy profiles along Lines 14 and 15, only four more detect layers >3.0 km below the seafloor, with the deepest being 3.6 km (see sonobuoy L14S3 in Table 1, Supplementary Material). Maximum velocities detected along Lines 14 and 15 are generally 4400–5000 m/s, with L14S1 (8000 m/s) and L14S3 (5600 m/s) being the only exceptions. Consequently, contours of faster velocity (>5400 m/s) in the 2D velocity model for Lines 14 and 15 are constrained by two head wave detections along the scarp of the continental shelf (L14S1 and L14S3), and are unconstrained under the Northern Basin.

The 2D velocity model based on Lines 16 and 17 (Fig. 8) shows velocity contours that are approximately flat (3800 m/s and 4400 m/s at ∼1.8 km and ∼2.2 km below the seafloor, respectively, or ∼2.3 and 2.7 km below sea level), and a shallow ve-

locity contour that is deflected downward in the middle of the line (2300 m/s, which ranges from 0 km to ∼0.5 km below the seafloor). The northwesternmost end of this velocity model is constrained by a relatively fast velocity at the seafloor (2800 m/s) and a relatively slow velocity for a depth of 1.4 km (3000 m/s; see L17S2 in Table 1, Supplementary Material); these detections deflect velocity contours away from their otherwise relatively smooth lateral horizons (Fig. 8).

Velocity contours in the 2D velocity model along Line 19 (Supplemental Fig. S4) are flat, depicting horizons with velocities up to 4500 m/s (at ∼2.5 km below the seafloor). These contours are in agreement with the model derived from Lines 16 and 17, and both are in good agreement with their crossing points on the model derived from Lines 14 and 15. Individual sonobuoy profiles along Line 19 record maximum velocities of 4100–4600 m/s at <3.0 km below the seafloor, representative of most sonobuoy data in the Northern Basin (see Table 1, Supplementary Material).

4. Discussion

4.1. Adare Basin

Sonobuoy L12S1 on the west end of Transect 1 (Fig. S2a) and the four along Line 9 (Fig. 5a–d) demonstrate the overall character on both sides of the Adare Trough of simple crustal structure (i.e., few layers) and shallow fast-velocity layers. In comparison, south of the trough the deep crustal structure is more complex (i.e., sonobuoys detect more layers), with deeper fast-velocity layers (e.g., Figs. 4b–d, S3a, S3c). This suggests thinner and less tectonically deformed crust along the flanks of the trough than in the portion of the Adare Basin between the trough and the Northern Basin. Previously deployed sonobuoys (Cooper et al., 1987) corroborate this interpretation, with a velocity of 5200 m/s detected at 1.8 km subseafloor depth just east of our Transect 1 and at 2.8 km subseafloor depth further south, just east of Line 13 (see Section 1.3).

Adjacent sonobuoy profiles along Line 13, in the southern Adare Basin, detect four to six layers, with similar maximum depths (2.7–3.5 km below the seafloor), and maximum velocities indicative of intrusive rock (5400–6600 m/s). These fast velocities suggest basement rock and perhaps lower oceanic crust (i.e., gabbro, typically 6000–7000 m/s; e.g., Jones, 1999, p. 64) at relatively shallow depths below the seafloor. Similar layer velocities at even shallower depths on either side of the Adare Trough (1.3–2.3 km below the sea floor) suggest continuity of oceanic crustal structure throughout the Adare Basin, with less overlying sedimentary material in the north than in the south. Horizontal velocity contours interpolated along Line 13 (Fig. 6) suggest that the deep north–south structure on the east side of the Adare Basin consists of laterally continuous layers, with little to no deformation.

However, Transects 1–3 reveal variation in deeper crustal structure throughout the basin. Basement rock is overlain by a thicker stack of sediments along the axis of the trough (Fig. S2b) than on its flanks (Figs. S2a and S2c), along the trend of Transect 1. This transect is not within the isopach contours of sediment thickness as determined in the Adare Basin using NBP0701 MCS data, but the trend of greater sediment thickness within the trough than on its flanks holds true south of Transect 1 (see Fig. 13c in Granot et al., 2010).

Further south, Transect 2 reveals structural asymmetry. The low velocity upper crustal layers (2000–4000 m/s) are thicker (by ∼0.3 km) west of the Adare Trough (Fig. S3a) than on its eastern side (Figs. S3b and S3c), with the slowest-velocity layers (2000–3000 m/s) significantly thicker (by ∼0.8 km) to the west. These results are consistent with sediment thicknesses determined from MCS data (Granot et al., 2010) at the locations of the

sonobuoys along Transect 2. Velocities of ~6000 m/s at ~1.8 km and ~2.3 km below the seafloor also show that fast crustal velocities are relatively shallow to the west and east of the southernmost extent of the Adare Trough, where it changes azimuth (Figs. S3a and b, respectively).

At the southernmost extent of the Adare Basin, along the base of the continental shelf, the middle sonobuoy in Transect 3 (L12S6) detects a layer velocity of 5300 m/s at 4.3 km below the seafloor, while sonobuoy profiles on either end of the transect detect a slightly faster velocity at slightly shallower depths (5700 m/s, at 4.1 km depth to the west and 2.8 km depth to the east). The greater depth of fast velocity layers along this transect than in the Adare Basin in general could be related to young volcanism clustered along the west side of the Adare Basin, just west of Transect 3 (see Fig. 12a in Granot et al., 2010). Alternatively, the greater depth of fast velocity layers along Transect 3 (particularly at sonobuoys L8S2 and L12S6, see Fig. 4) may be due to a thicker sedimentary package than in the rest of the Adare Basin. MCS data from NBP0701 show faulting in the shallow crust from ~17 Ma that follows the trend of the Adare Trough axis south to the continental shelf (Granot et al., 2010). This zone of deformation roughly coincides with the thickest Adare Basin sediments imaged with the MCS data (Granot et al., 2010), and its edges approximately correspond to the locations of sonobuoys L8S2 and L12S6. It may be that the general trend of thicker crust under the axis of the Adare Trough and thinner crust in the flanking portions of the Adare Basin (Müller et al., 2005) holds as far south as the continental shelf edge.

Having variable depths for velocities >5500 m/s, and velocities of 7000–7400 m/s (indicative of lower oceanic crust) in three locations at fairly shallow depths (in sonobuoys L2S2, L7S1, and L7S2; see Figs. 5e and S3c for the latter two), suggests variation in crustal thickness throughout the Adare Basin. The detections of 7000+ m/s velocities suggest that this crust is oceanic, as expected from water depth.

4.2. Structure across the continental shelf break

Three features stand out in the crustal structure across the margin between the Adare and Northern Basins (Fig. 7). One is the horizontal trend of deep velocity contours (5400–7000 m/s) along the first ~40 km of Line 14, beneath the water depths of ~2000–1500 m that lie adjacent to the continental shelf break. The second is the overall 1% grade of shallow velocity contours (2600–3700 m/s) from deep water to shallow, along the full length of Lines 14 and 15 (~125 km). These two trends in velocity contour depth are in contrast to the greater change in water depth along the lines, from 1960 m at L14S1 to ~500 m on the continental shelf (see Table 1, Supplementary Material). The small change in shallow velocity contour depth and lack of change in deep velocity contour depth suggest a continuity of crustal type across the continental shelf; velocity contours would have a larger change, and in the opposite direction (from shallow velocity contours), if the crust were to transition from oceanic to continental (e.g., Jones, 1999, p. 391). Continuity between Adare and Northern Basin crust is also suggested by two wide linear magnetic anomalies along the sides of the Northern Basin, which appear to be extensions of anomalies 16–18 on either side of the Adare Trough (Fig. 2b) (Cande and Stock, 2006), and by the absence of features in the Bouguer gravity anomaly data at the shelf break (Fig. 2c) (Davey et al., 2006).

Extensional deformation focused within the Adare Basin spreading center was more distributed within the adjacent continental crust to the south, either (locally) between the brittle crust of the Adare and Northern Basins and the underlying more ductile lithosphere (Davey et al., 2006), or (regionally) between the Northern Basin and other basins further east in the Ross Sea (Decesari et

al., 2007; Wilson and Luyendyk, 2009). The former predicts >100% stretching of the crust beneath the Northern Basin, whereas the latter expects the full amount of extension to be spread across three north–south bands of extension (the Northern Basin being the north end of the westernmost of these bands). Our study cannot resolve which of these is more accurate (i.e., what the stretching factor is for crust beneath the Northern Basin), but it does support the general idea of it being a transitional crustal type, as argued by Davey et al. (2006).

The third feature of interest in Fig. 7 is the maximum velocity of 8000 ± 100 m/s detected by L14S1, a value routinely interpreted as uppermost mantle (i.e., the location of the Moho). Measuring this velocity at 5.5 ± 0.4 km below the seafloor may be due to thin crust at this location (e.g., Selvans et al., 2012), or may be due to a planar interface within the basement rock that is significantly tilted (>10°) up toward the Northern Basin (see Section 3.2). If the true maximum velocity detected with sonobuoy L14S1 is 7900 m/s (within measurement uncertainty), it is also possible that the interface is in fact the Moho, but is composed of serpentinized mantle such as is observed in the Svalbard continental margin (Ritzmann et al., 2004).

Although no previous studies of crustal thickness along this portion of the Ross Sea continental shelf exist, some estimates of crustal thickness have been made within each basin using gravity data to determine Moho depth. Models of mantle Bouguer anomalies in the Adare Basin indicate crustal thicknesses of 9–10.5 km along the Adare Trough axis and 5–6 km east of the trough (Müller et al., 2005). This estimate of crustal thickness is consistent with our calculated value of 5.5 km, indicating that the crustal structure at the shelf break may be continuous with that of the Adare Basin, again suggesting a transitional crustal structure at the continental shelf break.

4.3. Northern Basin

This study indicates that the Northern Basin is filled with approximately horizontal sediment horizons (Figs. 7, 8, and S4), consistent with MCS data (Granot et al., 2010; Brancolini et al., 1995). Sediment layers potentially extend to a depth of >3 km, if maximum velocities of 4100–5000 m/s can be attributed to relatively fast-velocity sedimentary rock (consistent with interpretation of similar velocities, and basement depths of up to 3.0 km, to the south and east of our study; Cooper et al., 1987; Houtz and Davey, 1973). This is similar to the uppermost 3 km of crustal structure imaged in the western portion of Transect 3, at the base of the continental shelf (Fig. 4). Fast-velocity sediments and shallow bathymetry could be attributed, at least in part, to seaward propagation of glacio-marine sediment deposits that have filled the basin, out over oceanic crust, since its formation (e.g., Granot et al., 2013).

Two exceptions to the generally horizontal velocity contours observed in the Northern Basin are a slight down-warping of the 2300 m/s contour along the axis of the basin and close to the continental shelf (see Fig. 7), and a nearly constant velocity of ~2900 m/s for the entire 1.4 km depth of crust imaged by sonobuoy L17S2 (Fig. 8). Additionally, neighboring sonobuoy L16S6 (Fig. 8) detects layer interfaces to an anomalously shallow maximum depth (only 1.0 km below the seafloor) compared to the rest of the sonobuoy profiles in the Northern Basin. Interestingly, the linear magnetic anomaly along the west side of the Northern Basin (see Fig. 2b) corresponds to the location of sonobuoys L17S2 and L16S6.

Cande and Stock (2006) suggest that these magnetic anomalies may be the result of massive intrusions that helped accommodate extension in the Northern Basin. It is also possible that the crystalline crust of the Northern Basin is either oceanic crust or
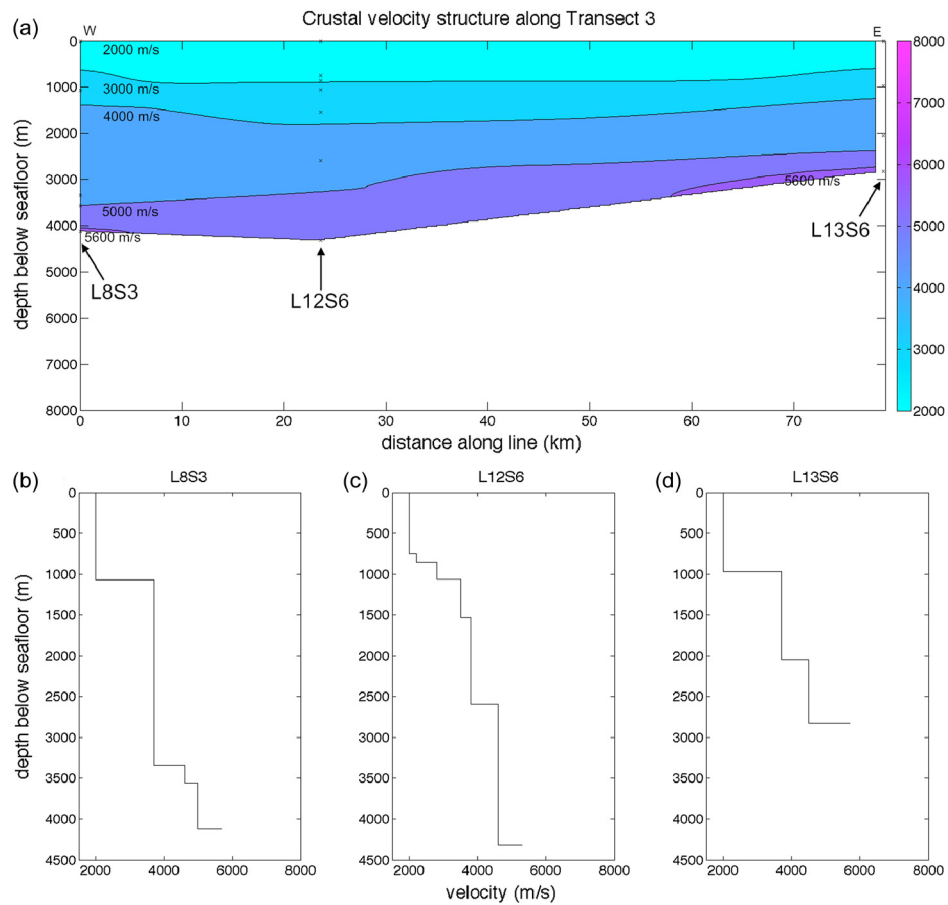
Fig. 4. 2D velocity model along Transect 3 (a) shows velocity contours based on interpolation between three 1D velocity models (b–d). Note that the shallow velocity contours (2000–4000 m/s) are relatively flat, while the 5000 m/s contour dips down to the west and the 5600 m/s contour is deflected down in the middle. Sonobuoys L8S3 (b) and L12S6 (c) detect the deepest layers with velocities <6000 m/s in the Adare Basin. Depths of individual layers directly detected in the sonobuoy data are plotted (with an "x") at the three sonobuoy positions; arrows point at the deepest layer detected by each sonobuoy. The velocity model is accurate for ±5 km along the line at each sonobuoy location; velocities are uncertain to ±100 m/s, depths up to ±0.4 km (increasing with depth).
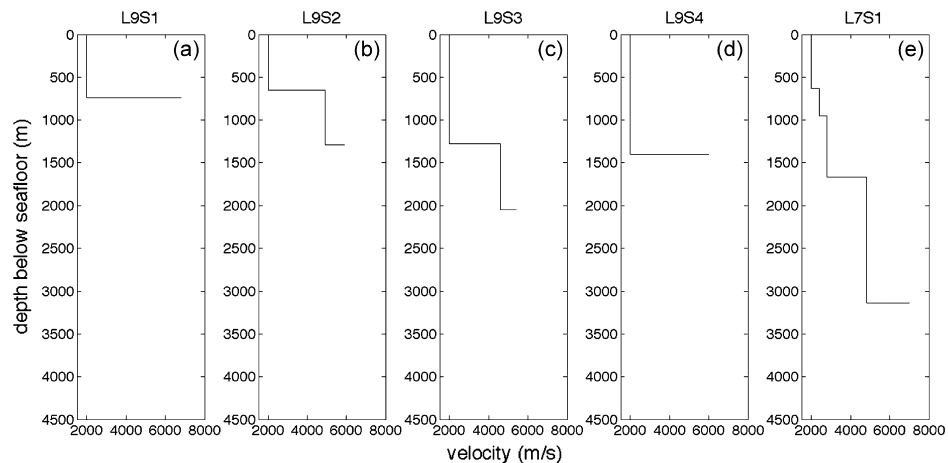

Fig. 5. From north to south (a)–(e), sonobuoy profiles along the east flank of the Adare Trough have maximum layer velocities of 6800 m/s, 5900 m/s, 5400 m/s, 6000 m/s, and 7000 m/s (respectively), the first four at relatively shallow depths compared to all sonobuoy profiles in the Adare Basin. Sonobuoy L7S1 (e) is one of three to detect a layer velocity >7000 m/s in the Adare Basin.

a transitional crust (Davey et al., 2006), as also inferred between oceanic and continental crust in the Gulf of California (Oskin et al., 2001). The shallow penetration depths of L17S2 and L16S6 may indicate disrupted crust, a likely occurrence either during massive intrusions associated with crustal extension or during more localized volcanic activity.

On the contrary, Davey and Brancolini (1995) interpret the deep Northern Basin structure as continental crust stretched by >100%. An estimate of Northern Basin crustal thickness, using gravity and seismic data to respectively determine Moho and basement depths, indicates ∼12 km of crystalline crust underlies sedimentary rock (Davey and Brancolini, 1995). If the Northern Basin is underlain
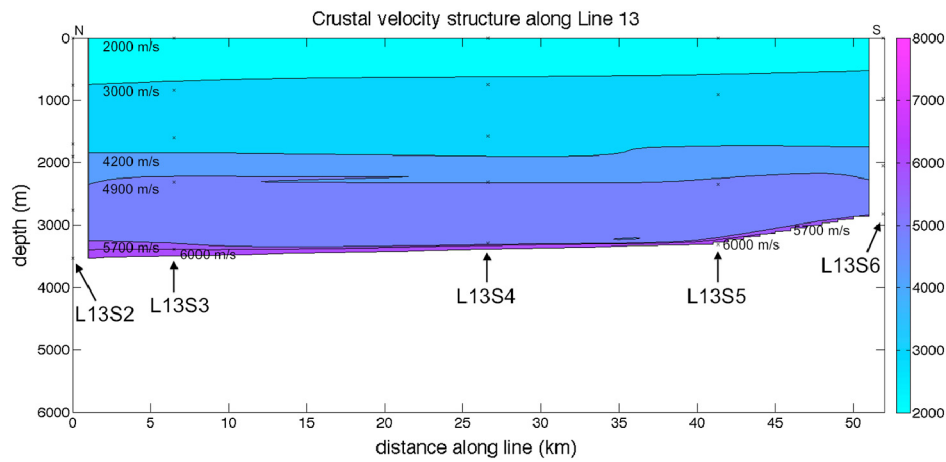
Fig. 6. 2D velocity model along Line 13 shows velocity contours based on interpolation between five adjacent 1D velocity models (see Table 1 in Supplementary Materials). Note that velocity contours are horizontal. Details of labeling and measurement uncertainty are as stated for Fig. 3; in this case, the model is accurate along the entire line.
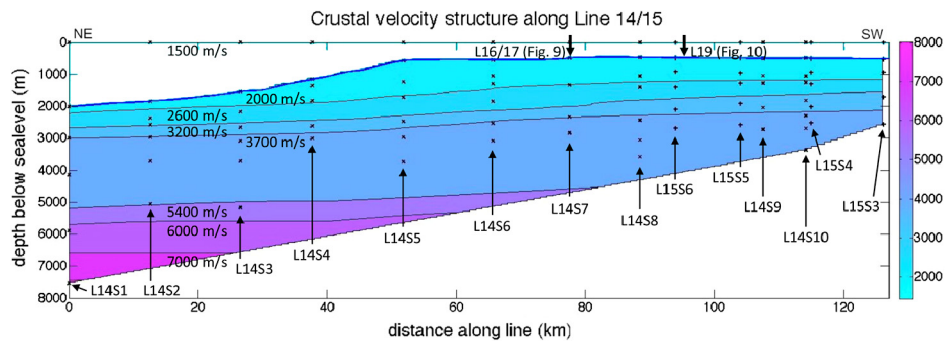

Fig. 7. 2D velocity model along Lines 14 and 15, which crosses the continental shelf from the Adare Basin to the Northern Basin (water layer in white). Velocity contours are based on interpolation between fourteen adjacent 1D velocity models. Note that velocity contours from 5400 m/s to 7000 m/s are approximately horizontal, and those from 2600 m/s to 3700 m/s have a shallow upward slope (∼1% grade overall) from deep ocean to shallow water depths. Contours are consistent with those at the southern end of Line 13 (Fig. 6). Depths of individual layers directly detected in the sonobuoy data ("x" for Line 14, "+" for Line 15) indicate the positions of the sonobuoys; arrows point at the deepest layer detected by each sonobuoy. Velocities are uncertain to ±100 m/s, depths up to ±0.4 km (increasing with depth).
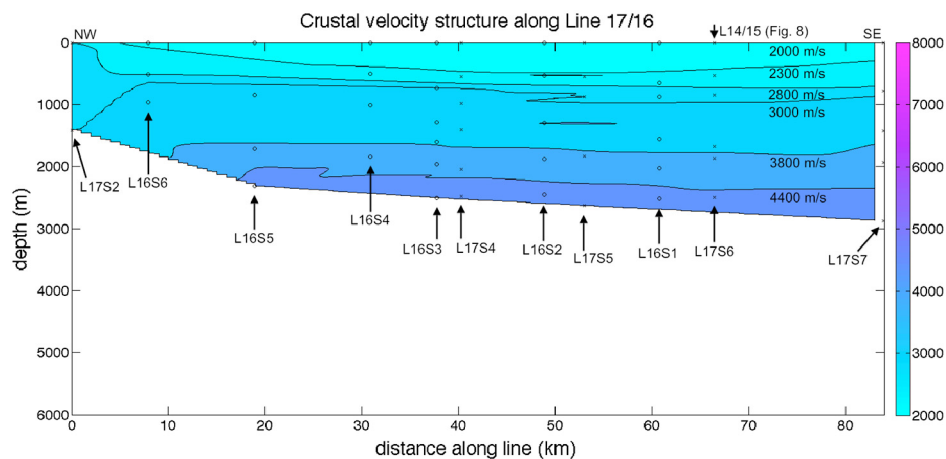

Fig. 8. A 2D velocity model along Lines 16 and 17 (a) in the Northern Basin shows velocity contours based on interpolation between eleven adjacent 1D velocity models. Note that velocity contours are generally horizontal, and reveal a crustal structure consistent with Lines 14 and 15 (Fig. 7) where they cross. Details of labeling and uncertainty are as stated for Fig. 7, with the exception that individual layers are labeled "x" for Line 17 and "o" for Line 16.
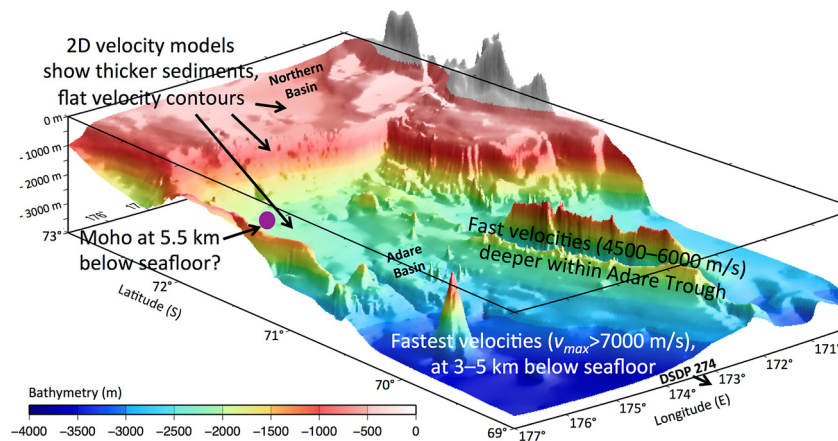
Fig. 9. Summary of results from sonobuoy analysis, shown with regional bathymetry (perspective is from the northeast). 1D velocity profiles east of the Adare Trough (in the Adare Basin) reveal velocities indicative of lower crust at relatively shallow depths, whereas the trough itself has fast velocities located deeper in the crust. Adjacent sonobuoys near the shelf break and in the Northern Basin show thicker sediment and flat velocity contours at depth, consistent with a continuous crustal type across the shelf. A potential Moho detection is located in near the shelf break.

by continental crust, it may be that the transition in crustal type between the Adare and Northern Basins occurs south of the shelf break.

The shallow subsurface structure of the Northern Basin as determined by this study (to ∼3 km depth) is consistent with previous seismic studies in the Ross Sea, as compiled and interpolated by Cooper et al. (1995). Those studies also revealed the uppermost of the sediment horizons to be nearly flat in the portion of the basin studied during research cruise NBP0701. Cooper et al. (1995) determined that the acoustic basement is almost entirely >4.0 km below the seafloor in this region (consistent with our deep velocity contours across the continental shelf; see Fig. 7), with a maximum of ∼5.5 km and a minimum of 2.0–3.0 km (the latter at the northwest extreme of the study area, approximately where sonobuoys L17S2 and L16S6 are located). However, our velocity contours do not directly correspond to the interfaces mapped by Cooper et al. (1995), because the RSU4a and RSU5 unconformities cross up into the eastern portions of our 2D velocity models for Line 17/16 (Fig. 8) and Line 19 (Fig. S4). It could be that sediment velocities in the Northern Basin are determined more by overburden pressure (i.e., depth) than by age, in which case previous seismic results and those of NBP0701 would be fully consistent.

4.4. Comparison to similar crust around the world

Ultraslow spreading zones such as the Adare Basin (∼12 mm/yr full-spreading rate; Cande et al., 2000) are typically associated with thin oceanic crust. The traditional view of oceanic crustal structure was determined from studies of ophiolite suites on land and marine seismic data, both of which indicated subhorizonal layering beneath the sediment–basement contact of 1) basaltic pillow lavas ($v_p \sim 5000$ m/s), 2) sheeted dikes, 3) gabbro ($v_p \sim 7000$ m/s), and 4) peridotite mantle ($v_p \sim 8000$ m/s), with mean oceanic crust (composed of basalt and gabbro) being ∼7 km thick (e.g., Christensen, 1978). However, in situ studies of these layers reveal that the oceanic crustal structure is complex and variable (Karson, 1998; Dick et al., 2003). Fault scarps on the seafloor reveal deviations from mean oceanic crustal structure on the scale of tens of meters to tens of kilometers, particularly along slow spreading ridges and in magma-poor locations, where stretching and thinning of the lithosphere often results in crust <7 km thick and the presence of oceanic core complexes (exposed along low-angle detachment faults, where rock units are missing, and contacts between units that are neither horizontal or continuous) (Karson, 1998).

Peridotites are found along ultraslow (≤12 mm/yr) spreading ridges (Dick et al., 2003), indicating that even mantle rock can be exhumed in these situations. Modeling of the detachment faulting process and resulting crustal thickness at spreading ridges, based on differing amounts of tectonic and magmatic crustal formation in both the upper (basalt) and lower (gabbro) oceanic crust (Olive et al., 2010), indicates that our measured crustal thickness of 5.5 km at the continental margin (2.1 km sediment and 3.4 km basement rock) is consistent with the formation of an oceanic core complex along a detachment fault at a slow-spreading ridge, in the case where half of the extension is accommodated through crustal thinning and half through magmatism (see summary Fig. 9). The fast velocities we measure at shallow depths along the eastern side of the Adare Trough (6000–7400 m/s, originating at 1–3 km below the seafloor) are also consistent with scenarios of oceanic core complex formation as modeled by Olive et al. (2010).

The crust around the arctic Gakkel Ridge (6–13 mm/yr full-spreading rate) reduces to thicknesses of 1.9–3.3 km along the ridge (Jokat et al., 2003), while thicknesses of 2.5–5.4 km (Minshull et al., 2006; Müller et al., 2000) are observed along the Southwest Indian Ridge (11–18 mm/yr; Chu and Gordon, 1999). Crustal thickness within the Adare Basin is not directly measured in this study, but thin oceanic crust would be consistent with the crustal structure detected by sonobuoy profiles along Lines 9 and 13 (Figs. 5 and 6), as well as sonobuoys L7S1 and L7S2 (Figs. 5e and S3c), where fast crustal velocities (up to 7400 m/s) are detected at relatively shallow depths in the crust. Adare Basin crust appears to be similar to that of oceanic core complexes observed and modeled at ultraslow spreading ridges (e.g., Karson, 1998).

5. Conclusions

Sonobuoy data in the Adare Basin suggest particularly thin oceanic crust along the east flank of the Adare Trough, consistent with estimates of 5–6 km thickness based on gravity data (Müller et al., 2005). Sonobuoy profiles also suggest the crust is thicker within the Adare Trough and along the base of the continental shelf, again consistent with Müller et al. (2005). Detection of a velocity of 8000 ± 100 m/s, which may have originated from the Moho at 5.5 ± 0.4 km below the seafloor, suggests that typical Adare Basin crustal thicknesses of 5–6 km could extend as far south as the continental shelf.

Adjacent sonobuoy profiles from the Adare Basin to within 12 km of the continental shelf break reveal deep velocity structure with horizontal contours, suggesting that the deep crustal structure of the Northern Basin may be continuous with that of the

Adare Basin. Further supporting evidence for the idea of continuous crustal structure between the basins includes magnetic anomalies that cross the continental shelf break (Cande and Stock, 2006), the continuous positive Bouguer gravity anomaly across the shelf (Davey et al., 2006), and fast velocity layers at greater depths from north to south within the Adare Basin.

Unfortunately, sonobuoy profiles within the Northern Basin do not detect velocities >5000 m/s or deeper than ~3 km subseafloor, and so mainly illustrate the horizontal velocity contours of the sedimentary rock filling the basin. The northwesternmost sonobuoy profiles in the Northern Basin are anomalous in terms of how shallowly they penetrate the crust, which may be due to disruption of sediments by massive intrusions.

By using the results of this study (Fig. 9) to constrain crustal velocity structure, analysis of shipboard gravity and multibeam bathymetry collected during research cruise NBP0701 may better constrain crustal thickness throughout the Adare and Northern Basins. However, in order to image the Moho in this area and determine whether the Northern Basin lies on top of stretched continental crust, transitional crust (including massive intrusions), or oceanic crust, it will be necessary to use an ocean-bottom seismic experiment to gain greater depth penetration than was realized in this study.

Acknowledgements

Appendix A. Supplementary material

Supplementary material related to this article can be found online at http://dx.doi.org/10.1016/j.epsl.2014.08.029. These data include the Google maps of the most important areas described in this article.

References

Adare Basin Sonobuoy Data, 2007. Sonobuoy Data from the Adare Basin, Antarctica. California Institute of Technology, dataset http://dx.doi.org/10.7909/C37P8W9P, http://www.gps.caltech.edu/~clay/Adare_Sonobuoy/Adare_Sonobuoy.html.

Becker, J., Sandwell, D., 2006. SRTM30_PLUS: SRTM30, coastal & ridge multibeam, estimated topography. Electronic journal. http://topex.ucsd.edu/WWW_html/srtm30_plus.html.

Brancolini, G., Cooper, A.K., Coren, F., 1995. Seismic facies and glacial history in the western Ross Sea (Antarctica). Antarct. Res. Ser. 68, 209–233.

Bruns, T., Carlson, P., 1987. Geology and petroleum potential of the southeast Alaska continental margin. In: Geology and Petroleum Potential of the Continental Margin of Western North America and Adjacent Ocean Basins–Beaufort Sea to Baja California. Houston, TX. In: Earth Science Series, p. 269.

Cande, S.C., Stock, J.M., 2004. In: Exon, N.F., Kennett, J.K., Malone, M.J. (Eds.), Cenozoic Reconstruction of the Australia–New Zealand–South Pacific Sector of Antarctica. AGU, Washington, DC, pp. 5–18.

Cande, S.C., Stock, J.M., 2006. Constraints on the timing of extension in the Northern Basin, Ross Sea. In: 9th International Symp. on Antarctic Earth Sci. Proceedings.

Cande, S.C., Raymond, C.A., Stock, J., Haxby, W.F., 1995. Geophysics of the Pitman Fracture Zone and Pacific–Antarctic plate motions during the Cenozoic. Science 270 (5238), 947.

Cande, S.C., Stock, J.M., Müller, R.D., Ishihara, T., 2000. Cenozoic motion between east and west Antarctica. Nature 404 (6774), 145–150.

Christensen, R.B., 1978. Ophiolites, seismic velocities and oceanic crustal structure. Tectonophysics 47, 131–157.

Chu, D., Gordon, R.G., 1999. Evidence for motion between Nubia and Somalia along the Southwest Indian Ridge. Nature 398 (6722), 64–67.

Cochrane, G.R., De Santis, L., Cooper, A.K., 1995. Seismic velocity expression of glacial sedimentary rocks beneath the Ross Sea from sonobuoy seismic-refraction data, Geology and Seismic Stratigraphy of the Antarctic Margin. In: Antarctic Research Series, vol. 68, pp. 261–270.

Cooper, A.K., Davey, F.J., 1985. Episodic rifting of Phanerozoic rocks in the Victoria land Basin, western Ross Sea, Antarctica. Science 229 (4718), 1085.

Cooper, A.K., Davey, F.J., Cochrane, G.R., 1987. Structure of extensionally rifted crust beneath the western Ross Sea and Iselin Bank, Antarctica, from sonobuoy seismic data. In: The Antarctic Continental Margin: Geology and Geophysics of the Western Ross Sea. In: Earth Science Series. Circum-Pacific Council of Energy and Mineral Resources, Houston, TX, pp. 93–117.

Cooper, A.K., Barker, P.F., Brancolini, G. (Eds.), 1995. Geology and Seismic Stratigraphy of the Antarctic Margin. Antarctic Research Series, vol. 68. Maps 16b, 18b, 18d, 22a-d.

Damaske, D., Laufer, A.L., Goldmann, F., Moller, H.-D., Lisker, F., 2007. Magnetic anomalies northeast of Cape Adare, northern Victoria Land (Antarctica), and their relation to onshore structures. In: 10th International Symp. on Antarctic Earth Sci. Proceedings.

Davey, F., Brancolini, G., 1995. The late Mesozoic and Cenozoic structural setting of the Ross Sea region. In: Geology and Seismic Stratigraphy of the Antarctic Margin, pp. 167–182.

Davey, F.J., Bennett, D.J., Houtz, R.E., 1982. Sedimentary basins of the Ross Sea, Antarctica. N.Z. J. Geol. Geophys. 25, 245–255.

Davey, F.J., Hinz, K., Schroeder, H., 1983. Sedimentary basins of the Ross Sea, Antarctica. In: Anarctic Earth Science. Australian Academy of Science, Canberra, pp. 533–538.

Davey, F.J., Cande, S.C., Stock, J.M., 2006. Extension in the western Ross Sea region-links between Adare Basin and Victoria Land Basin. Geophysical Research Letters 33, L20315. http://dx.doi.org/10.1029/2006GL027383.

Decesari, R.C., Wilson, D.S., Luyendyk, B.P., Faulkner, M., 2007. Cretaceous and Tertiary extension throughout the Ross Sea, Antarctica. Related publications from ANDRILL Affiliates. Paper 11, http://dx.doi.org/10.3133/of2007-1047.srp098.

Dick, H.J.B., Lin, J., Schouten, H., 2003. An ultraslow-spreading class of ocean ridge. Nature 426 (6965), 405–412.

Elliot, D.H., 1992. Jurassic magmatism and tectonism associated with Gondwanaland break-up: an Antarctic perspective. Geol. Soc. (Lond.) Spec. Publ. 68 (1), 165.

Gaina, C., Müller, D.R., Royer, J.Y., Stock, J., Hardebeck, J., Symonds, P., 1998. The tectonic history of the Tasman Sea: a puzzle with 13 pieces. J. Geophys. Res. 103 (B6), 12,413–12,433.

Gardner, G., Gardner, L., Gregory, A., 1974. Formation velocity and density of the diagnostic basics for stratigraphic traps. Geophysics 39, 770.

Geissler, W.H., Jokat, W., 2004. A geophysical study of the northern Svalbard continental margin. Geophys. J. Int. 158 (1), 50–66.

Granot, R., Cande, S., Stock, J., Davey, F., Clayton, R., 2010. Postspreading rifting in the Adare Basin, Antarctica: regional tectonic consequences. Geochem. Geophys. Geosyst. 11 (8), Q08005.

Granot, R., Cande, S.C., Stock, J.M., Damaske, D., 2013. Revised Eocene–Oligocene kinematics for the West Antarctic rift system. Geophys. Res. Lett. 40. http://dx.doi.org/10.1029/2012GL054181.

Hayes, D.E., et al., 1975a. Site 274. DSDP Initial Rep. 28, pp. 369–433. http://dx.doi.org/10.2973/dsdp.proc.28.110.1975.

Hayes, D.E., et al., 1975b. Site 273. DSDP Initial Rep. 28, pp. 335–367. http://dx.doi.org/10.2973/dsdp.proc.28.109.1975.

Houtz, R., Davey, F., 1973. Seismic profiler and sonobuoy measurements in Ross Sea, Antarctica. J. Geophys. Res. 78 (17), 3448–3468.

Jokat, W., Ritzmann, O., Schmidt-Aursch, M., Drachev, S., Gauger, S., Snow, J., 2003. Geophysical evidence for reduced melt production on the Arctic ultraslow Gakkel mid-ocean ridge. Nature 423 (6943), 962–965.

Jones, E.J.W., 1999. Marine Geophysics. Wiley.

Karson, J.A., 1998. Internal structure of oceanic lithosphere: a perspective from tectonic windows. In: Buck, R. (Ed.), Faulting and Magmatism at Mid-Ocean Ridges, pp. 177–218.

Luyendyk, B., Cisowski, S., Smith, C., Richard, S., Kimbrough, D., 1996. Paleomagnetic study of the northern Ford Ranges, western Marie Byrd Land, West Antarctica: motion between West and East Antarctica. Tectonics 15 (1), 122–141.

Minshull, T.A., Müller, M.R., White, R.S., 2006. Crustal structure of the Southwest Indian Ridge at 66°E: seismic constraints. Geophys. J. Int. 166 (1), 135–147.

Molnar, P., Atwater, T., Mammerickx, J., Smith, S.M., 1975. Magnetic anomalies, bathymetry and the tectonic evolution of the South Pacific since the Late Cretaceous. Geophys. J. R. Astron. Soc. 40 (3), 383–420.

Müller, M., Minshull, T., White, R., 2000. Crustal structure of the Southwest Indian Ridge at the Atlantis II fracture zone. J. Geophys. Res. 105 (B11), 25809–25828.

Müller, R.D., Cande, S.C., Stock, J.M., Keller, W.R., 2005. Crustal structure and rift flank uplift of the Adare Trough, Antarctica. Geochem. Geophys. Geosyst. 6 (11).

NBP0701 Data Report, 2007. Prepared by J. Ayers, http://www.marine-geo.org/tools/search/data/field/NBPalmer/NBP0701/docs/NBP0701Report.htm.

Olive, J.A., Behn, M.D., Tuckolke, B.E., 2010. The structure of oceanic core complexes controlled by the depth distribution of magma emplacement. Nat. Geosci. 3 (7), 491–495.

Oskin, M., Stock, J., Martìn-Barajas, A., 2001. Rapid localization of Pacific–North America plate motion in the Gulf of California. Geology 29 (5), 459.

Panter, K.S., Castillo, P., 2007. Petrogenesis and source of lavas from seamounts in the Adare Basin, Western Ross Sea: implications for the origin of Cenozoic magmatism in Antarctica. Paper presented at 10th International Symposium on Antarctic Earth Sciences.

Ritzmann, O., Jokat, W., Czuba, W., Guterch, A., Mjelde, R., Nishimura, Y., 2004. A deep seismic transect from Hovgärd Ridge to northwestern Svalbard across the continental ocean transition: a sheared margin study. Geophys. J. Int. 157 (2), 683–702.

Sandwell, D.T., Smith, W.H.F., 2009. Global marine gravity from retracked Geosat and ERS-1 altimetry: ridge segmentation versus spreading rate. J. Geophys. Res. 114, B01411. http://dx.doi.org/10.1029/2008JB006008.

Selvans, M.M., Clayton, R.W., Stock, J.M., Granot, R., 2012. Using overlapping sonobuoy data from the Ross Sea to construct a 2D deep crustal velocity model. Mar. Geophys. Res. 133 (1), 17–32.

Tréhu, A., Behrendt, J., Fritsch, J., 1993. Generalized crustal structure of the Central basin, Ross Sea, Antarctica. Geol. Jahrb., Reihe E Geophys. 47, 291–311.

Trey, H., Cooper, A.K., Pellis, G., della Vedova, B., Cochrane, G., Brancolini, G., Makris, J., 1999. Transect across the West Antarctic rift system in the Ross Sea, Antarctica. Tectonophysics 301 (1–2), 61–74.

Truswell, E.M., Drewry, D.J., 1984. Distribution and provenance of recycled palynomorphs in surficial sediments of the Ross Sea, Antarctica. Mar. Geol. 59 (1–4), 187–214.

Weaver, S., Storey, B., Pankhurst, R., Mukasa, S., DiVenere, V., Bradshaw, J., 1994. Antarctica–New Zealand rifting and Marie Byrd Land lithospheric magmatism linked to ridge subduction and mantle plume activity. Geology 22 (9), 811.

Wilson, D.S., Luyendyk, B.P., 2009. West Antarctic paleotopography estimated at the Eocene–Oligocene climate transition. Geophys. Res. Lett. 36, L16302. http://dx.doi.org/10.1029/2009GL039297.